CIMAC CONGRESS 25
ZURICH, MAY 19 – 23, 2025

2025 | 167

Cashew nutshell liquid as a biofuel: use of additives to improve engine operability

Fuels - Alternative & New Fuels

Amy Bates, Infineum

Thomas Marsden, Infineum

ABSTRACT

There are several challenges associated with the use of cashew nutshell liquid (CNSL) as a marine biofuel, primarily resulting from its high level of unsaturation and tendency to polymerize at high temperatures. Such polymerization generates lacquer-like deposits which block injector nozzles and inhibit fuel injection into the combustion chamber. Infineum has conducted bench and engine tests to investigate the mechanisms behind lacquer formation and assess the efficacy of fuel additives in mitigating these problems.

The primary areas of investigation were blends of CNSL with VLSFO. High-temperature polymerisation experiments and particle size measurements demonstrated that polymerised CNSL (polycardanol) interacts strongly with asphaltenes and promotes deposit formation. The performance of anti-polymerisation and cleanliness additives was subsequently validated in a single-cylinder four-stroke engine. As a result of this test program, engine operability with CNSL-derived biofuel blends was improved via the development of a bespoke marine fuel additive package.

1 INTRODUCTION

In accordance with the targets set by the International Maritime Organisation (IMO), the shipping industry is required to significantly reduce its greenhouse gas (GHG) emissions and become carbon-neutral by 2050 [1]. A variety of measures will be implemented in order to achieve these targets, relating to (for example) ship machinery, exhaust gas aftertreatment, logistics and digitalisation. However, the most direct route to carbon neutrality will be via the use of alternative fuels, and whilst options like ammonia and hydrogen are longer-term prospects, drop-in biofuels can deliver significant interim benefits.

1.1 Production and Composition of Cashew Nutshell Liquid (CNSL)

An emerging drop-in marine biofuel is cashew nutshell liquid (CNSL). CNSL is a caustic, viscous oil which is extracted from cashew nutshells after the nuts have been harvested. The chemical composition of the oil may vary, depending on both the source of the cashew tree and the extraction method.

Cold extraction of the raw cashew nut shell (mechanical or solvent extraction) is performed at a maximum temperature of 60 °C and produces 'natural' CNSL (n-CNSL). The oil comprises multiple components of which the primary constituent is anacardic acid (60-70%, Figure 1). Alternatively, roasting cashew nutshells at higher temperatures of 150-190 °C produces 'technical' CNSL (t-CNSL), in which the anacardic acid decarboxylates to produce an oil consisting predominantly of cardanol (60-65%) [2,3]. T-CNSL can be further distilled to remove impurities and increase the proportion of cardanol, generating a product suitable for industrial applications.

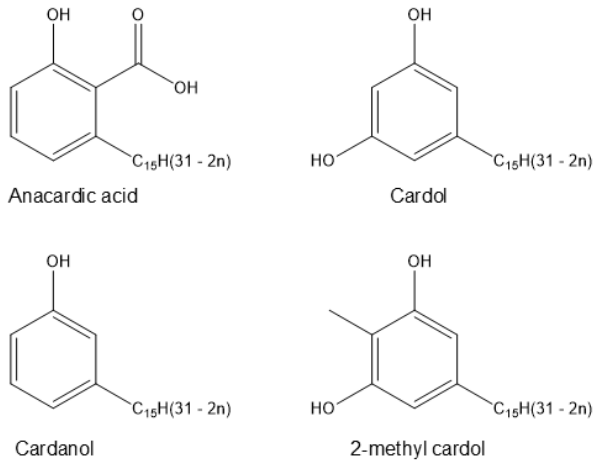

Figure 1: Constituents of CNSL [2].

Cardanol describes a mixture of components with variable degrees of unsaturation in the alkyl chain. The saturated, mono-, di- and triolefinic species may be separated by liquid-liquid extraction and other methods documented in the literature [4]. The chemical profile of cardanol enables it to be used in a variety of applications such as antioxidants and surfactants, and to undergo polymerisation reactions to produce thermoplastics and resins with excellent corrosion, heat and chemical resistance. Cardanol-based polymers are used extensively for industrial applications, such as paints and coatings, plasticisers, adhesives and even food and beverages [4].

1.2 Advantages and Challenges of CNSL as a Marine Biofuel

The use of CNSL as a marine biofuel presents several advantages, both from an environmental and an economic perspective. In addition to the widely-understood benefits of biofuels, whereby the feedstocks consume carbon dioxide (CO_2) from the atmosphere and hence offset the environmental impact of combustion, CNSL has the advantage of being derived from agro-industrial waste products (nutshells). Consequently, its use as a fuel reduces waste and promotes resource efficiency [5]. CNSL offers an advantage over biofuels which compete for feedstocks used for food production, such as ethanol, and can also be priced favourably relative to conventional fuels and other biofuels. This is an additional incentive for its use in the maritime industry.

From an operational perspective, CNSL readily combines with conventional marine fuels such as very low sulfur fuel oil (VLSFO) and marine gasoil (MGO), typically in up to a 30% ratio, without requiring modifications to vessel infrastructure. Within these fuel blends, the highly oxygenated species present in CNSL have been shown to improve combustion efficiency and reduce carbon monoxide (CO) and hydrocarbon (HC) emissions [6].

Conversely, there are factors which need to be carefully considered when using CNSL as a marine biofuel. The toxic and highly sensitising nature of CNSL presents challenges with handling and storage, and the global supply is unreliable and limited by weather and processing capacity. From the perspective of the fuel delivery system, the polymerisation of cardanol at elevated temperatures produces lacquer-type deposits which block fuel injector nozzles [7]. This may occur to the extent where fuel is unable to enter the combustion chamber and consequently, the engine becomes inoperable. Further investigation into the mechanism(s) of deposit formation, lacquer composition and development of preventative

measures is required, in order to facilitate engine operability.

This paper explores the fundamental mechanisms behind deposit formation in blends of CNSL with conventional marine fuels. High-temperature polymerisation experiments, particle size measurements and engine tests have been used to investigate these processes and design chemical additive solutions for improving engine operability.

2 EXPERIMENTAL

2.1 Blend Preparation

VLSFO was blended with CNSL or polycardanol (as required) on a hotplate with stirring, at a temperature of 60 C for 30 minutes.

2.2 Heating Experiment

A sample (up to 50 g) of cardanol (95% purity, Combi-Blocks Inc.), CNSL or a blend of CNSL and VLSFO was weighed into a three-necked round-bottomed flask (RBF) fitted with a reflux condenser and a nitrogen blanket. A steel coupon, cleaned via sonication in toluene for 15 minutes, was placed in the RBF to act as a surface for deposition. After 10 minutes' purging with nitrogen, the RBF was heated to 225 °C for four days (9am-5pm), with the temperature reduced to 210 °C overnight for safety purposes. The products were analysed via Gel Permeation Chromatography (GPC), Infrared Spectroscopy (IR) and Nuclear Magnetic Resonance (NMR) to confirm that polymerisation had taken place.

2.2.1 Gel Permeation Chromatography (GPC)

The sample of interest was diluted to the required concentration using tetrahydrofuran (THF) and analysed using an Agilent 1200 chromatograph. The chromatograph used an Agilent PolarGel column and a mobile phase of toluene (1%) in THF. Polystyrene standards of known molecular weight were used to calculate the molecular weights of cardanol and polycardanol.

2.2.2 Infrared Spectroscopy (IR)

Materials were analysed using a PerkinElmer Spectrum Two FT-IR spectrometer.

2.2.3 ^{1}H Nuclear Magnetic Resonance (NMR)

The sample of interest was diluted to the required concentration (ca. 1 wt.%) using chloroform-d and analysed using a Bruker 300 MHz spectrometer. The results were analysed using ACD/Labs Spectrus software.

2.3 Asphaltene Dispersancy Test (ADT)

The fuel of interest (0.5 mL) was mixed with toluene (0.5 mL) and pipetted into a 100 mL volumetrically graduated glass centrifuge tube. 100 mL n-heptane was added and the tube stoppered with a cork. The tube was immediately inverted three times, in order to ensure homogeneous mixing, and then placed in a stability rack in front of a backlight. A camera was used to record timelapse footage of asphaltene deposition.

2.4 Dynamic Light Scattering (DLS)

The fuel of interest (50 uL) was mixed with toluene (50 uL) and then diluted with heptane (2000 uL). The sample was placed into a sealed quartz cuvette and shaken to ensure homogeneity. The sample was then placed into a Malvern Zetasizer and analysed using the instrument's built-in software.

2.5 Particle Size Measurements: LUMiSizer®

The fuel of interest (10 uL) was mixed with toluene (10 uL) and then diluted with heptane (400 uL). The sample was poured into a low density polyethylene (LDPE) cuvette and shaken to ensure homogeneity. The sample was then placed into a LUM GmbH LUMiSizer®, which uses centrifugation and laser transmittance to determine a particle size distribution.

The LUMiSizer typically images particles up to 5 µm, but was modified in order to accommodate larger particle sizes. The position of a particle is related to its diameter through the modified version of the Stokes Equation below:

$$x^2 = \frac{18\,\eta \ln\left(\frac{r_m}{r_0}\right)}{\vec{g}\,\Delta\rho\,t_m}$$

where x = particle diameter,

η = dynamic viscosity of the liquid phase,

r_m = measurement position from the centre of rotation,

r_0 = meniscus position from the centre of rotation,

$\vec{g}$ = gravitational force experienced by the particle, that is:

$$\vec{g} = 11.2 \cdot r_{centrifuge} \cdot \left(\frac{rpm}{1000}\right)^2$$

Δp = density difference between the continuous and dispersed phases, that is:

$$\Delta\rho = \rho_{solid} - \rho_{liquid}$$

and t_m = time of measurement.

The cumulative distribution function for particle size was calculated using an extinction-weighted constant position approach, which forces r_m to remain constant. At a position of 117.0 mm along the cuvette, the meniscus was observed at 108.7 mm. The cumulative distribution function of particle size is displayed below:

$$Q(x_i) = \frac{1}{2} \cdot (f_i + g_{i-1,i}) \cdot E_i + \sum_{j=1}^{i-1} \left(\frac{f_i + g_{i-1,i}}{g_{j+1,i} + g_{j,i}} - \frac{f_i + g_{i-1,i}}{g_{j,i} + g_{j-1,i}} \right) \cdot Q_j$$

where, considering i as the time of measurement during the current iteration:

$$f_i = \left(\frac{r_m}{r_0}\right)^2$$

$$g_{i,j} = f_i^{\left(\frac{x_i}{x_j}\right)^2}$$

for an i , j, $1, 2, 3, \ldots, j \leq i$ and $i, j \in \mathbb{N}^+$

$$g_{0,i} = 1 \; and \; g_{i,i} = f_i$$

and

$$E_i = -\ln\left(\frac{T}{T_0}\right)$$

where T_0 = transmittance at time T = 0.

3 RESULTS AND DISCUSSION

3.1 Fundamental Mechanisms Behind Deposit Formation

This section explores the fundamental mechanisms behind deposit formation of CNSL / VLSFO blends in fuel injector nozzles.

3.1.1 Polymerisation of Cardanol

Three distinct methods for the polymerisation of cardanol can be found in the literature [8, 9, 10]. These are i) addition polymerisation, ii) Friedel-Crafts polymerisation and iii) etherification. All three mechanisms can be catalysed by metals or salts present in the fuel blend (Figure 2).

Addition polymerisation involves the temperature-induced homolytic cleavage of a double bond in the alkyl chain, followed by radical attack on another double bond in the alkyl chain of a second cardanol molecule. This chain growth mechanism continues until a polymer is formed and terminates when two radicals collide. Conversely, the Friedel-Crafts mechanism involves temperature-induced heterolytic cleavage of a double bond in the alkyl chain, followed by electrophilic attack of the aromatic ring by the resulting ion. The etherification mechanism involves nucleophilic attack of the hydroxy group on a double bond to form an ether.

In order to identify the predominant mechanism of cardanol polymerisation at high temperature, cardanol was heated to 225 °C for four days (Section 2.2) and the product analysed via GPC, IR and ^{1}H NMR. The integration of GPC IR response data indicated that approximately 47% of the starting material was converted to polycardanol, (Table 1). Analysis of the IR spectra (Figure 3) revealed a stretching pattern at ca. 3300 cm^{-1}, which is representative of the hydroxy (-OH) group. Considering a 47% conversion rate and since only a minor reduction in intensity of this peak was observed after heating, etherification was discounted as the predominant polymerisation mechanism. The ^{1}H NMR spectra displayed in Figure 4 also show no appearance of an ether signal (3-4.5 ppm).

Table 1: GPC data for cardanol, after heating.

Peak	Retention Time (min)	Area (nRIU*s)	Assignment
1	24.286	161,241	Polycardanol
2	24.878	178,668	Cardanol

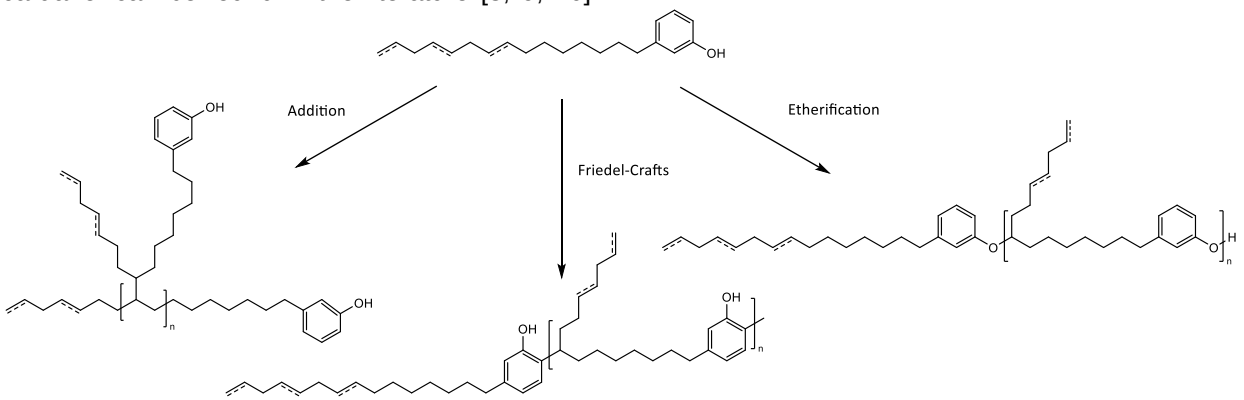

Figure 2: Polymerisation mechanisms of cardanol. Note that polymerisation can take place through any of the double bonds; the schemes shown above are examples.

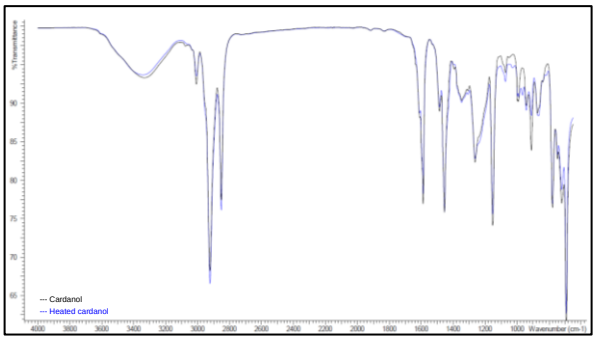

Figure 3: IR spectra of cardanol, before and after heating.

Similarly, the ^{1}H NMR data discredits the Friedel-Crafts polymerisation mechanism. The resonances between 6.5-7.5 ppm are representative of aromatic hydrogen environments [11] and remain unchanged in chemical shift and integration between the starting material and product (Figure 4). By process of elimination, it appears that temperature-induced polymerisation of cardanol proceeds predominantly via the addition mechanism. A control experiment was also performed on hydrogenated cardanol, containing no double bonds, and the ^{1}H NMR spectra displayed no change before and after heating (Figure 5).

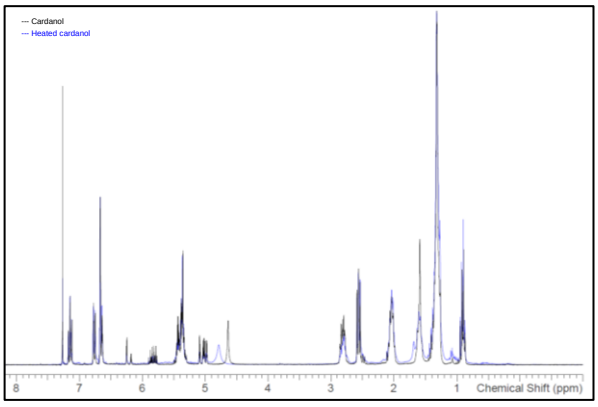

Figure 4: ^{1}H NMR spectra of cardanol, before and after heating.

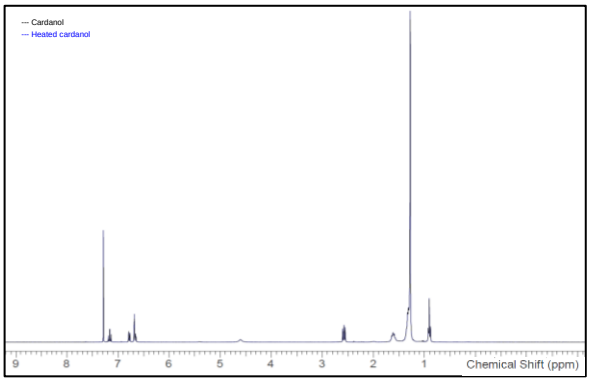

Figure 5: ^{1}H NMR spectra of hydrogenated cardanol, before and after heating.

It is important to note that whilst high temperatures evidently promote cardanol polymerisation via the addition mechanism, it is possible that impurities present in CNSL may also catalyse polymerisation via alternative mechanisms. For example, it was reported that an Fe/H_2O_2 catalyst system initiates cardanol polymerisation with no reaction of the unsaturated groups [12]. This could be further investigated by replicating the heating experiment on fuel blends containing CNSL in the presence of an Fe catalyst.

3.1.2 Interaction with Asphaltenes

The interaction of polycardanol with asphaltenes was studied via the Asphaltene Dispersancy Test (ADT), Dynamic Light Scattering (DLS) and LUMiSizer®. The polycardanol produced from the heating experiment in Section 3.1.1 was used in these studies.

Initially, a series of destabilisation experiments was conducted on different concentrations of VLSFO and polycardanol at a fixed total volume, using heptane to initiate asphaltene deposition. As the proportion of pre-heated cardanol in the blend increased from 0 to 30% (that is, up to approximately 14% polycardanol considering the conversion rate), a clear interaction between asphaltenes and polycardanol was observed (Figure 6). The resulting deposits did not settle in the bottom of the stability tube as in the blend without polycardanol, but adhered to the glass surface in a lattice-type structure. The particle sizes were visibly larger and perceived to drop out of solution more readily. A control experiment with 30% cardanol in VLSFO did not display the same behaviour.

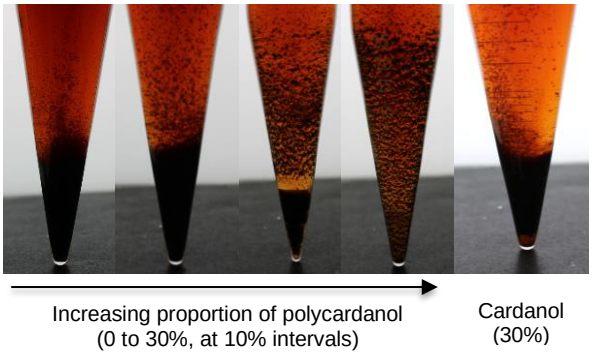

Figure 6: ADT results for blends of VLSFO and polycardanol.

The sizes of the deposits were subsequently quantified via DLS (Figure 7). As observed visually in the ADT, an increasing proportion of polycardanol results in a larger average particle diameter, increasing linearly from 1142 nm to 1853 nm as the proportion of heated cardanol increases from 0 to 30% of the total volume. Since the

addition polymerisation of cardanol preserves its phenolic head groups and hence allows them to rotate freely, the increased particle size is attributed to co-ordination of these head groups with asphaltene moieties, via hydrogen bonding, pi-pi stacking and Van der Waals' forces [13]. Additionally, the increased weight percentage of co-ordinating heteroatoms 'activates' the asphaltenes, such that deposits adhere to surfaces more readily. In this respect, the resulting species may be compared to interfacially active asphaltenes [14].

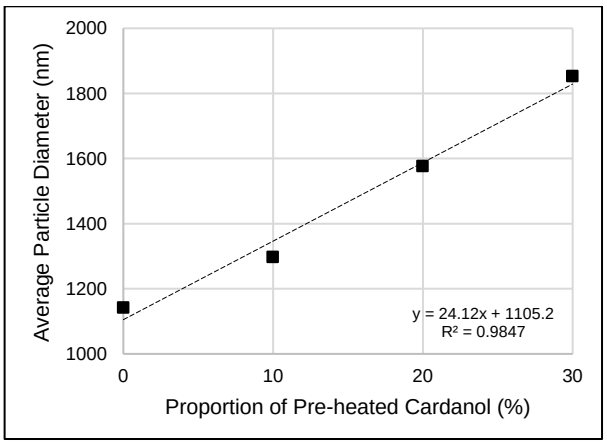

Figure 7: DLS results for blends of VLSFO and polycardanol.

The LUMiSizer® uses a constant shear environment to stimulate asphaltene deposition on the micrometer scale, facilitating analysis of colloidal aggregation. The data obtained (Figure 8) reinforce the idea that deposits on this scale become larger with an increasing concentration of polycardanol.

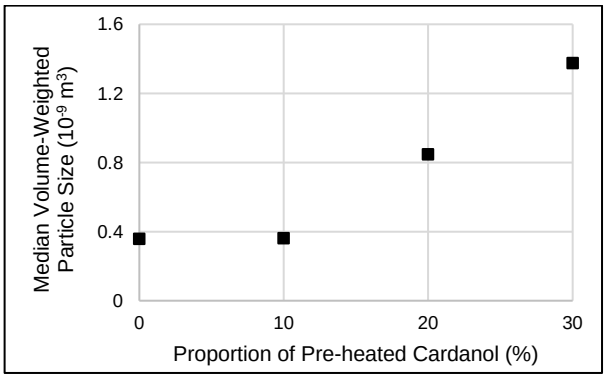

Figure 8: LUMiSizer® results for blends of VLSFO and polycardanol.

As displayed above, aggregates containing polycardanol are larger than typical asphaltene aggregates, and there appears to be a linear relationship between particle size and polycardanol concentration. These polycardanol-containing aggregates have a greater surface area available for interaction with other asphaltenes, which may pack more densely around them. Consequently, it is possible that deposits of reduced polydispersity and tighter molecular packing are able to interact with surfaces more strongly.

3.2 Additive Solutions to Engine Operability Problems

When operating a marine engine on a blend of CNSL and VLSFO, the lacquering observed in injector nozzles may be explained by the effects detailed in Section 3.1.2. Since asphaltenic species are too heavy to vapourise during fuel injection, they deposit in the injector nozzles. The high temperatures polymerise the CNSL constituents, which then readily bind to the asphaltenes. Whilst the pressure of fuel injection is able to disperse these deposits to an extent, they gradually accumulate to produce a hard, strongly adhered lacquer.

It is interesting to note that lacquering is observed predominantly in injector nozzles, rather than elsewhere in the fuel delivery system. Whilst it is possible that carbon steel present in tanks and pipes acts as an Fe catalyst and promotes cardanol polymerisation via mechanisms other than addition, since lacquering is not prevalent in other areas of the fuel delivery system, it is unlikely that steel alone is able to initiate polymerisation. Whether Fe plays a role or not, we can conclude that a high temperature is the principal requirement for cardanol polymerisation and lacquering.

With a greater understanding of the mechanisms of cardanol polymerisation and lacquering, it was hypothesised that chemical additives could be used to reduce deposition from blends of CNSL and VLSFO on injector nozzles and hence improve engine operability. This could be achieved by i) disrupting the addition polymerisation process and ii) disrupting the co-ordination mechanism. Considering these approaches, Additive A was developed and its performance validated in a static engine test.

A four-stroke, single cylinder engine (SCE) was operated using a blend of degummed t-CNSL (30%) and VLSFO (70%), denoted 'C30'. During an initial test with no additive, deposits formed on the injector nozzle (Figure 9) and interfered with the fuel spray, to the extent where an increased injection duration was required to deliver the fuel to the combustion chamber. Consequently, the centre of combustion was delayed and the exhaust temperature increased.

In order to compensate for the increased exhaust temperature and maintain a safe operating window,

the injection pressure was increased and the injection timing advanced. However, at the highest loads these measures were insufficient to reduce the exhaust temperature, such that a safety cut-out was activated and the engine was rendered inoperable. The highest load which could be reached with the baseline fuel is indicated in Figure 10.

Figure 9: Injector nozzle following engine operation without additive (LHS) and with Additive A (RHS).

When a fuel blend treated with Additive A was tested, fewer deposits built up on the injector nozzle and improved combustion characteristics were observed. The Specific Fuel Oil Consumption (SFOC), Filter Smoke Number (FSN) and concentration of CO emissions were substantially reduced at all engine loads (Figures 10-12). It is important to note that the fuel injection timing and pressure were altered as described previously, in order to maintain a safe operating window. Whilst the injection parameters were not necessarily identical for both fuels at a given load, the engine was able to reach 100% load with additised fuel and so we can conclude that Additive A facilitated engine operability.

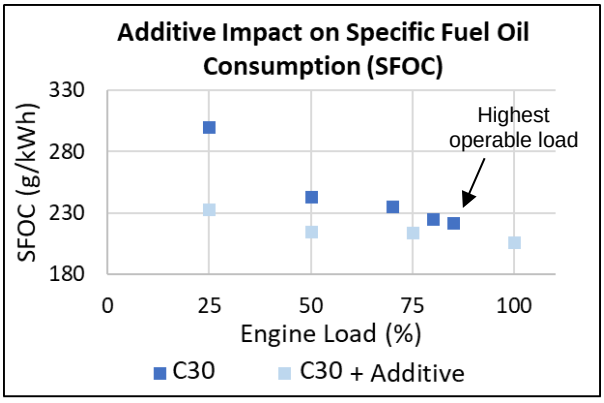

Figure 10: Impact of Additive A on SFOC.

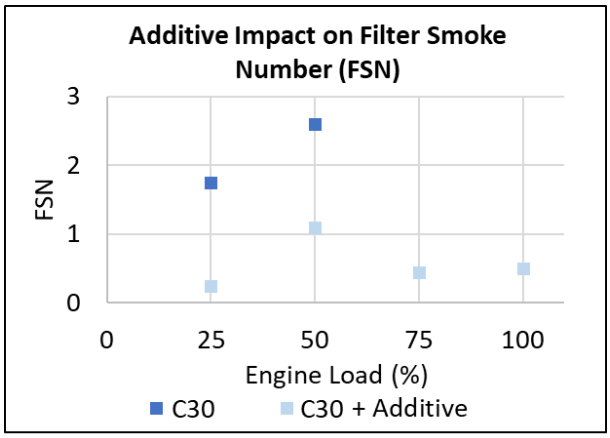

Figure 11: Impact of Additive A on FSN.

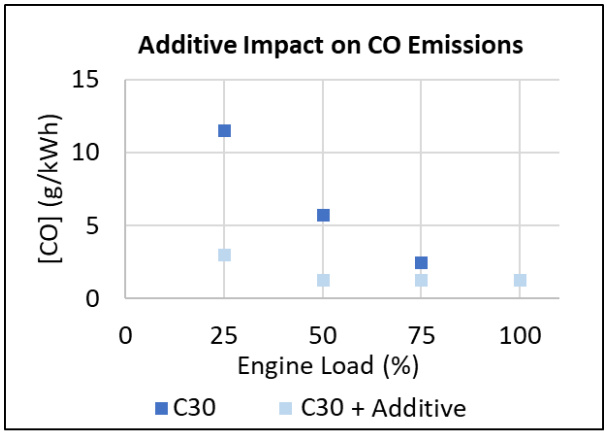

Figure 12: Impact of Additive A on CO emissions.

Additive A maintained a cleaner condition of the injector nozzles (Figure 9), enabling fuel to be more effectively injected into the combustion chamber. The additive can also be expected to deliver cleanliness benefits to the remainder of the fuel delivery system. The learnings from this paper have been implemented in the modification of bench tests, which can be used to further improve the additive package going forwards.

4 CONCLUSIONS

The fundamental mechanisms behind deposit formation in blends of CNSL with conventional marine fuels, and the use of chemical additive solutions for improving engine operability, were investigated. The primary constituent of t-CNSL, cardanol, was polymerised at high temperature and the mechanism deduced by analysing the product (polycardanol) via IR and ^{1}H NMR. Polymerisation proceeded via the addition mechanism, where the temperature-induced homolytic cleavage of a double bond in the alkyl chain generates a radical, which subsequently attacks another double bond in the alkyl chain of a second cardanol molecule.

Asphaltene destabilisation and particle size measurements were then used to investigate the interaction of polycardanol with asphaltenes. It was observed that an increasing proportion of polycardanol blended with VLSFO generated larger deposits when destabilised, due to the co-ordination of the phenolic head groups with asphaltene moieties. It was also proposed that the increased heteroatom content of polycardanol 'activates' the asphaltenes, enabling them to adhere to surfaces more readily and produce a hard lacquer.

Finally, Additive A was successfully developed to interrupt the cardanol polymerisation mechanism and enable aggregates to pass through to the combustion chamber, rather than deposit on injector nozzles. Additive A was blended into a mixture of CNSL (30%) and VLSFO (70%) and tested in a static single cylinder engine. The combustion characteristics of the engine were notably improved with additive, with SFOC, FSN and CO appearing to be greatly reduced. The engine was able to safely operate at 100% load which was not possible for the baseline fuel.

Going forwards, the additive package can be further improved in terms of chemistry and treat rate, in order to maximise engine performance benefits. It is important to note that CNSL falls outside of the ISO 8217:2024 marine fuel standard and requires Class Society and OEM engagement to enable its commercial use. Additive development will continue with a view to enabling CNSL to be successfully used as a transitional fuel on IMO's decarbonisation pathway.

5 DEFINITIONS, ACRONYMS, ABBREVIATIONS

CNSL: Cashew nutshell liquid

n-CNSL: Natural cashew nutshell liquid

t-CNSL: Technical cashew nutshell liquid

VLSFO: Very low sulphur fuel oil

CO: Carbon monoxide

GPC: Gel Permeation Chromatography

IR: Infrared Spectroscopy

NMR: Nuclear Magnetic Resonance

ADT: Asphaltene Dispersancy Test

DLS: Dynamic Light Scattering

SFOC: Specific fuel oil consumption

FSN: Filter smoke number.

6 ACKNOWLEDGEMENTS

The authors would like to acknowledge Lloyd's Register for their support with this research.

7 REFERENCES AND BIBLIOGRAPHY

[1] International Maritime Organisation, 2023, Revised GHG Reduction Strategy for Global Shipping Adopted, *www.imo.org*.

[2] Gedam, P.H. and Sampathkumaran, P.S., 1986, Cashew Nut Shell Liquid: Extraction, Chemistry and Application, *Progress in Organic Coatings*, 14, 115-157.

[3] Santos Andrade, T. *et. al.*, 2011, Antioxidant Properties and Chemical Composition of Technical Cashew Nut Shell Liquid (tCNSL), *Food Chemistry*, 126, 1044-1048.

[4] Bhatia, B. *et. al.*, 2024, Isolation of Cardanol Fractions from Cashew Nutshell Liquid (CNSL): A Sustainable Approach, *Sustainable Chemistry*. 5, 68-80.

[5] Lomonaco, D. *et. al.*, 2017, *Cashew Nut Shell Liquid: A Goldfield for Functional Materials*, Springer International Publishing, Cham, Switzerland.

[6] Tamilselvan, P. *et. al.*, 2017, A Comprehensive Review on Performance, Combustion and Emission Characteristics of Biodiesel Fuelled Diesel Engines, *Renewable and Sustainable Energy Reviews*, 79, 1134-1159.

[7] International Institute of Marine Surveying, 2024, Cashew Nutshell Marine Biofuel Warning Sent Out, *www.iims.org.uk*.

[8] Voirin, C. *et. al.*, 2014, Functionalisation of Cardanol: Towards Biobased Polymers and Additives, *Polymer Chemistry*, 5, 3142-3162.

[9] Qian, W. *et. al.*, 2022, Synthesis of Linear Poly-cardanol and its Application in Rubber Materials, *Express Polymer Letters*, 16(1), 75-84.

[10] Bai, W. *et. al.*, 2012, Synthesis and Characterisation of Cross-linked Polymer from Cardanol by Solvent-free Grinding Polymerisation, *Progress in Organic Coatings*, 75(3), 184-189.

[11] Hoang, A.S. *et. al.*, 2015, Synthesis of Oxime from a Renewable Resource for Metal Extraction, *Korean Journal of Chemical Engineering*, 32(8), 1598-1605.

[12] Ikeda, R. *et. al.*, 2000, A New Crosslinkable Polyphenol from a Renewable Resource, *Macromolecular Rapid Communications*, 21, 496-499.

[13] Celia-Silva, L.G. *et. al.*, 2020, Preaggregation of Asphaltenes in the Presence of Natural Polymers by Molecular Dynamics Simulation, *Energy and Fuels*, 34, 1581-1591.

[14] Ballard, D.A. *et. al.*, 2020, Aggregation Behaviour of E-SARA Asphaltene Fractions Studied by Small-Angle Neutron Scattering, *Energy and Fuels*, 34(6), 6894-6903.